



Published in final edited form as:

*Alzheimers Dement.* 2021 May ; 17(5): 847–855. doi:10.1002/alz.12241.

## Utility of MRI in the identification of hippocampal sclerosis of aging

Davis C. Woodworth<sup>1,2</sup>, Hannah L. Nguyen<sup>3</sup>, Zainab Khan<sup>3</sup>, Claudia H. Kawas<sup>1,2,4</sup>, María M. Corrada<sup>1,2,4,5</sup>, S. Ahmad Sajjadi<sup>1,2</sup>

<sup>1</sup>Department of Neurology, University of California, Orange, California, USA

<sup>2</sup>Institute for Memory Impairments and Neurological Disorders, University of California, Irvine, California, USA

<sup>3</sup>Department of Biological Sciences, University of California, Irvine, California, USA

<sup>4</sup>Department of Neurobiology and Behavior, University of California, Irvine, California, USA

<sup>5</sup>Department of Epidemiology, University of California, Irvine, California, USA

### Abstract

**Introduction:** Hippocampal sclerosis of aging (HS) is a common pathology often misdiagnosed as Alzheimer's disease. We tested the hypothesis that participants with HS would have a magnetic resonance imaging (MRI)-detectable hippocampal pattern of atrophy distinct from participants without HS, both with and without Alzheimer's disease neuropathology (ADNP).

**Methods:** Query of the National Alzheimer's Coordinating Center database identified 198 participants with MRI and autopsy. Hippocampal subfields were segmented with FreeSurfer v6. Analysis of covariance for subfield volumes compared HS+ participants to those without HS, both with ADNP (HS-/ADNP+) and without (HS-/ADNP-).

**Results:** HS+ participants (N = 27, 14%) showed atrophied cornu ammonis 1 (CA1; left  $P < .001$ ,  $\eta_p^2 = 0.14$ ; right  $P = .001$ ,  $\eta_p^2 = 0.09$ ) and subiculum (left  $P < .001$ ,  $\eta_p^2 = 0.139$ ; right  $P = .001$ ,  $\eta_p^2 = 0.085$ ) compared to HS-/ADNP+ (N = 100, 51%). Compared to HS-/ADNP- (N = 71, 36%), HS+ also had atrophy in subiculum (left  $P < .001$ ,  $\eta_p^2 = 0.235$ ; right  $P = .002$ ,  $\eta_p^2 = 0.137$ ) and CA1 (left  $P < .001$ ,  $\eta_p^2 = 0.137$ ; right  $P = .006$ ,  $\eta_p^2 = 0.070$ ).

**Discussion:** Subiculum and CA1 atrophy from clinical MRI may be a promising in vivo biomarker for HS.

### Keywords

Alzheimer's disease; atrophy; CA1; dementia; hippocampal sclerosis of aging; hippocampus; magnetic resonance imaging; subiculum

---

**Correspondence** S. Ahmad Sajjadi, Office 364, Med Surge II, Academy Way, Irvine, CA, 92697, USA. ssajjadi@uci.edu.

SUPPORTING INFORMATION

Additional supporting information may be found online in the Supporting Information section at the end of the article.

## 1 | BACKGROUND

Hippocampal sclerosis of aging (HS) is common and a significant contributor to dementia in older populations.<sup>1-3</sup> Pathologically, HS is characterized by gliosis and neuron death in the subiculum and cornu ammonis 1 (CA1) regions of the hippocampal formation.<sup>4</sup> While the prevalence of Alzheimer's disease (AD) neuropathology levels off with age, the prevalence of HS continues to rise and is present in up to 30% of nonagenarians who die with dementia.<sup>5</sup> Clinically, HS is often conflated with AD because of similar clinical profiles and the lack of *ante mortem* biomarkers for HS. However, to properly manage patients with HS or to exclude those suffering from HS from AD neuropathology-targeted clinical trials, *ante mortem* biomarkers of this neuropathological condition are much needed.

Most of the previous magnetic resonance imaging (MRI) studies in relation to HS have focused on the whole hippocampus. The aim of this study was to examine the utility of MRI in identifying hippocampal subfield atrophy with a focus on the regions associated with HS. We leveraged the neuropathology and MRI data available through the National Alzheimer's Coordinating Center (NACC) database to test the hypothesis that MRI-defined atrophy of subiculum and CA1 regions of the hippocampus can serve as a biomarker for HS and can help differentiate HS from its greatest mimic, AD neuropathology, during life.

## 2 | METHODS

### 2.1 | Participants

We used data from participants with and without dementia, who had both MRI and pathology data available in the NACC database (September 2005 to March 2017). The NACC Uniform Data Set (UDS) consists of data submitted by approximately 30 National Institute of Aging (NIA) funded Alzheimer's Disease Centers (ADCs) across the United States since 2005.<sup>6</sup> Contributing ADCs are each approved by their local institutional review board. This study used data from 11 ADCs.

### 2.2 | Neuropathology

Neuropathological data are collected at the ADCs via a standardized Neuropathology Form and Coding Guidebook.<sup>7</sup> The NACC pathology data dictionary was used to define pathological categories. HS was defined as present/absent (+/-) based on the HS-listed variables in different versions of the neuropathology data dictionary: NPHIPP-SCL (NACC version 10), categorizing HS as present or absent (+/-) in the CA1 and/or subiculum, and NPSCL (NACC version 9), categorizing medial temporal lobe sclerosis as present or absent (+/-) including hippocampal sclerosis. Alzheimer's disease neuropathology (ADNP) was considered present in those who met high likelihood NIA-Reagan criteria.<sup>8</sup> This comprised a combined Consortium to Establish a Registry for Alzheimer's Disease (CERAD) neuritic plaque score of 3 (Frequent) and high Braak stage for neurofibrillary tangles (V/VI: neocortical involvement extending to occipital lobe). We chose the high likelihood for our ADNP definition because this represents the highest burden and thus ostensibly the highest level of neurodegeneration, making it the most difficult to distinguish from HS. Additionally, to evaluate whether other pathologies may be related to the hypothesized hippocampal

atrophy signature of HS in a multiple linear regression model (see below), we considered the following neuropathologies: cerebral amyloid angiopathy (CAA): none/mild (–) and moderate/severe (+); Lewy bodies: available as present/absent (+/–); atherosclerosis: none/mild (–), moderate/severe (+); gross infarcts and lacunes: available as present/absent (+/–); microinfarcts available as present/absent (+/–), and hemorrhages and microbleeds available as present/absent (+/–). A few participants had missing data for some of the pathologies assessed (see Table 1). Our predefined groups of interest were those with HS regardless of ADNP (HS+), those with ADNP but without HS (HS–/ADNP+), and those without either HS or ADNP (HS–/ADNP–). It is noteworthy that the NACC database lacked information about TAR DNA-binding protein 43 (TDP-43) status on 161 of 198 (81%) of the participants in this study. Therefore, TDP-43 status and its relation to MRI findings could not be studied in this dataset.

### 2.3 | MRI

Our initial search identified 243 participants with both pathology and at least one MRI. Of these, 29 did not have a 3D T1w scan (having only 2D scans unsuitable for segmentation), and three did not have HS data, resulting in 211 participants with at least one 3D T1w scan and relevant pathology data. The 3D T1w scans were converted from DICOM to Nifti by the `dcm2nii` command from MRICron.<sup>9</sup> The Nifti images were then processed using the FreeSurfer (v6.0) `recon-all` command with default settings. Total intracranial volumes (TIV) from FreeSurfer were generated for use in analyses. Next the FreeSurfer Hippocampal Subfield Segmentation Module<sup>10</sup> was used to define the subfields of the hippocampal formation. All hippocampal subfield segmentations were inspected visually to ensure appropriate segmentation of the hippocampus from surrounding structures (cerebrospinal fluid, white matter, and brainstem). For scans that did not process correctly due to `recon-all` failure, alternative skullstrip or Talairach registration steps were performed. Thirteen participants were excluded due to incorrect hippocampal segmentations that could not be fixed (four HS+, seven ADNP+/HS–, one HS–/ADNP–) leaving 198 participants with usable data. For 62 participants who had multiple MRI sessions with suitable quality (22 HS–/ADNP–, 33 HS–/ADNP+, 7 HS–/ADNP–), we chose the MRI session closest to death to reduce time from scan to autopsy. Example segmentations for a representative participant from each group are shown in Figure S2 in supporting information. For comparison and validation of the FreeSurfer hippocampal subfield segmentations, we also processed the scans using the Automatic Segmentation of Hippocampal Subfields (ASHS) Penn Memory Center T1-Only Atlas for T1-weighted 3T MRI (PMC-T1) pipeline<sup>11</sup> as outlined in supporting information.

As expected, there was a wide variation in scanner vendor, model, and acquisition parameters for the 3D T1w scans. Most scans were acquired on a GE scanner (150, 76%), while 38 (19%) were acquired on a Siemens and 10 (5%) on a Philips. Most scans were on a 1.5T scanner (133, 67%), with the rest (65, 33%) acquired on a 3T scanner. Five different sequence paradigms were used in acquiring the data: GE scanners used either a spoiled gradient recalled echo (SPGR) that in some instances was accelerated (FSPGR), or with inversion recovery (IR-FSPGR), or a research magnetization prepared rapid acquisition gradient echo (MPRAGE<sup>12</sup>) sequence. Siemens MRIs were all acquired using an MPRAGE

sequence and Philips scans used a 3D turbo field echo (TFE) sequence (Figure S1 in supporting information). Averages and ranges of scan parameters for the various vendor and sequence combinations are shown in Table S1 in supporting information, and distributions of volumes by field strength, scan sequence, and scanner vendor are shown in Figure S3 in supporting information.

#### 2.4 | Demographic and clinical variables

We selected the following clinical variables for this study: sex, age at MRI, years from MRI to death, years of education, age at death, and dementia status at the neuropsychological assessments closest to MRI. Dementia status at the final visit and the percentage of participants with mild cognitive impairment (MCI) in those without dementia is also reported.

#### 2.5 | Statistical analysis

To examine whether atrophy of the hippocampal subfields was greater in participants with HS, we used analysis of covariance (ANCOVA) to compare hippocampal subfield volumes of interest between the groups (HS+ vs HS-/ADNP+, and HS+ vs HS-/ADNP-). We also performed an ANCOVA restricted to HS+ participants to examine whether ADNP or dementia was significantly associated with decreased volumes. We selected the hippocampal formation subfields subiculum and CA1 as our primary regions of interest; we additionally selected CA3, and CA4 as regions of interest, given their involvement in aging and AD. Figure 1A shows a diagram of these regions of interest. We also report analyses using the total hippocampal volume and the hippocampal tail—which is the posterior portion of the hippocampus unaffected by HS pathology—volume for comparison. All ANCOVA tests were performed accounting for sex, age at MRI, years between MRI and death, years of education, and dementia status at time of MRI. Marginal means and standard deviations of the volumes were also calculated for the different groups adjusting for the other covariates. Effect sizes in the form of partial eta-squared ( $\eta_p^2$ ) values were interpreted in accordance with Cohen,<sup>13</sup> where a  $\eta_p^2$  of 0.06 is moderate, and 0.14 is large.

To investigate whether MRI scan acquisition paradigm could affect group differences, we examined the effect sizes for the subiculum and CA1 regions in the ANCOVA models for the whole group as well as for smaller groups comprising more homogenous acquisition parameters. The first subset of analyses included scans that incorporated an inversion pulse (IR-FSPGR and MPRAGE, N = 129) and the second subset of analyses included only scans acquired using an MPRAGE sequence (N = 77). We chose inversion recovery sequences as previous studies have shown other parameters such as field strength,<sup>14</sup> averages,<sup>14</sup> and acceleration factors<sup>14, 15</sup> have a relatively minor effect on MRI volumetrics and are mostly related to the signal-to-noise ratio.

Finally, to examine whether additional common pathologies might influence the atrophy of the subiculum and CA1, we implemented a multiple linear regression to investigate the relation between total CA1 and subiculum volume (sum of CA1 and subiculum volumes across both hemispheres) and all available neuropathologies (including HS and ADNP) alongside the demographic covariates in the same model. For this multiple linear regression,

we excluded four participants who had incomplete neuropathology data (Table 1). For validation, we compared the subiculum and CA1 volume from FreeSurfer to the ASHS PMC-T1 segmentations of the anterior hippocampus through Pearson's correlation, and computed the multiple linear regression model for the ASHS PMC-T1 segmentations in addition to FreeSurfer.

## 2.6 | Data availability

NACC data are freely available to researchers upon request.

# 3 | RESULTS

## 3.1 | Participant characteristics

The characteristics for the groups are summarized in Table 1. There were 27 (14% of total) HS+, 100 (51%) HS-/ADNP+, and 71 (36%) HS-/ADNP- participants. The HS+ group was older at time of MRI and death. HS+ (4.4) and HS-/ADNP+ (3.9) participants had similar mean years from MRI to death, while this was shorter for HS-/ADNP- participants (maximum intervals between MRI and death: 10 years). There was a trend for higher proportion of females in the HS+ group (52%) compared to HS-/ADNP+ (34%). There were no significant between-group differences infrequency of other pathologies. Although the HS+ group had a lower proportion of dementia at the time of MRI (59%) compared to HS-/ADNP+ (87%), all the HS+ participants without dementia had MCI and were diagnosed with dementia at the visit closest to death. Within the HS+ group, approximately half of participants were also ADNP+ (52%). The prevalence of dementia at time of MRI was similar for the HS+/ADNP+ (64%) and HS+/ADNP- (54%) subgroups. Table S2 displays demographics for HS+ cases stratified by ADNP. Table S3 in supporting information displays the distribution of participants by group across the 11 contributing ADCs.

## 3.2 | Hippocampal subfield volumes for HS+ versus HS-/ADNP+

The HS+ group had significantly lower hippocampal subfield volumes compared to the HS-/ADNP+ group with moderate-to-large effect sizes (range of  $\eta_p^2$  for subiculum and CA1, 0.085–0.144), with the effect sizes larger for the left hemisphere (Figure 1C, Table 2). CA3 and CA4 also had significantly lower volumes in HS+ versus HS-/ADNP+, though the effect sizes were less than for the subiculum and CA1. The hippocampal tail was not significantly different between the HS+ and HS-/ADNP+ groups ( $P > .2$ ). In addition, the whole hippocampus was significantly smaller in the HS+ group compared to the HS-/ADNP+ group but the effect size was slightly lower than that of the subiculum and CA1 (Table 2).

## 3.3 | Hippocampal subfield volumes for HS+ versus HS-/ADNP-

The HS+ group had significantly lower hippocampal subfield volumes compared to the HS-/ADNP- group (range of  $\eta_p^2$  for subiculum and CA1, 0.101–0.253, again with effects larger in left hemisphere, Figure 1B and Table 2). However, the hippocampal tail was not significantly smaller in the HS+ compared to the HS-/ADNP- group ( $P > .3$ ). The whole hippocampus was also significantly decreased in volume in the HS+ group compared to the

HS-/ADNP- group but the effect size was slightly smaller than that of the subiculum and CA1 for each respective hemisphere (Table 2). Figure 2 displays the marginal means from the ANCOVA models for HS for both group comparisons, which illustrate the large effect of HS on subiculum and CA1 volumes compared to the small effects for the hippocampal tail.

### 3.4 | Associations within HS+ group

Within the HS+ group, we found no significant difference in hippocampal subfield volumes by either ADNP ( $P = .2$  for all regions of interest [ROIs]) or dementia ( $P = .2$  for all ROIs) status.

### 3.5 | Effect sizes for group comparisons with more homogeneous MRI acquisitions

Table 3 shows the effect sizes for the subsets of participants with more homogeneous MRI acquisition parameters. This restriction led to larger effect size estimates for most comparisons.

### 3.6 | Associations of pathologies and demographic variables with subiculum and CA1 volume

Last, studying the association between total subiculum/CA1 volume and degenerative pathologies (Table 4) we found HS was the only neuropathology that was significantly associated with lower CA1 and subiculum volume ( $t = -4.079$ ,  $P < .001$ ). Additionally, TIV ( $t = 4.208$ ,  $P < .001$ , larger volume with larger cranium), age at MRI ( $t = -3.142$ ,  $P = .002$ , decrease in volume with age), and dementia status ( $t = -4.642$ ,  $P < .001$ , lower volume in those with dementia) were also associated with the combined subiculum/CA1 volume. Pointedly, ADNP was not associated with subiculum/CA1 volume ( $t = -0.452$ ,  $P = .7$ ). To examine whether this was due to co-occurrence of dementia in this group, the multiple linear regression was implemented without dementia as a covariate, for which ADNP only trended toward significance ( $t = -1.955$ ,  $P = .052$ ), while the effect of HS remained strong ( $t = -3.900$ ,  $P < .001$ ). Anterior hippocampal volumes from ASHS PMC-T1 were highly correlated with the total subiculum/CA1 volume ( $r = 0.893$ ), and results for the multiple linear regression model using the anterior hippocampus (Table S3) were similar to those for the FreeSurfer total subiculum/CA1 (Table 4).

## 4 | DISCUSSION

In this study, we examined the utility of MRI in identifying an atrophy signature of hippocampal sclerosis, a common and less studied cause of dementia in those 85 years and older. We examined the volume of hippocampal subfields in participants with HS neuropathology compared to participants with and without ADNP using the NACC database. We found moderate-to-large effect size hippocampal atrophy comparing participants with HS to those without. In agreement with neuropathological characteristics of HS, we found the largest difference in subiculum and CA1 regions of the hippocampal formation. These effects were detected in a dataset with heterogeneous acquisition paradigms and the effect sizes generally increased when limiting the MRI scans to higher quality and more consistent acquisition subsets. We also found that HS was the only degenerative neuropathology that was associated with subiculum and CA1 atrophy.

The volume of the hippocampus is routinely used as a measure of neurodegeneration. One study found lower hippocampal volumes, as measured by MRI at time closest to death, for both HS and ADNP.<sup>16</sup> Another study found total hippocampal atrophy in those with HS compared to those with ADNP or no neuropathology, and also found surface deformations of the hippocampus in areas corresponding to the CA1 and subiculum regions.<sup>17</sup> Two *post mortem* MRI studies found lower hippocampal volumes<sup>18,19</sup> and contraction in hippocampal surfaces<sup>20</sup> in participants with HS compared to those without. However, to the best of our knowledge no studies have thus far examined the effect of HS on hippocampal subfield volumes (as opposed to total hippocampal volumes or surface deformations of the hippocampus) and directly compared HS to ADNP in that regard.

We focused on the subiculum and CA1 regions of hippocampal formation since atrophy and gliosis in these regions are what defines HS pathologically and indeed, we found the most atrophy in these regions. CA3 and CA4 regions also showed more atrophy in the HS group but there were no differences between groups with regard to the volume of the hippocampal tail. This indicates a pattern of atrophy in HS that is more prominent in the anterior portion of hippocampus or hippocampal head. Moreover, these results suggest that while the greatest degree of atrophy in HS is present in the subiculum and CA1, other regions are also displaying decreased volume. The previous MRI studies of *ante mortem*<sup>17</sup> and *post mortem*<sup>20</sup> hippocampal shape deformation in relation to HS found a general sparing of the outer surfaces of the CA3 and CA4 in HS participants. However, autopsy studies have shown CA3 and CA4 subfields do display a greater accumulation of TDP-43—the proteinopathy signature of HS—in brains with HS versus those without.<sup>21</sup> This accumulation of TDP-43 might lead to a degree of atrophy that can be picked up by more sensitive analysis of hippocampal subfields.

One perhaps unexpected finding from this study is the lack of an association between ADNP and CA1/subiculum volumes. Previous MRI studies of *ante mortem*<sup>17</sup> and *post mortem*<sup>20</sup> hippocampal shape deformation found that while HS had a larger effect, ADNP was also related to subiculum and CA1 atrophy. However, these studies did not account for dementia status at the time closest to the scan. Therefore, it is conceivable that the volume of these regions is tied more closely to dementia and less to ADNP: while removing the dementia variable from our models yielded a trend for ADNP, its effect was small compared to that of dementia. Other studies also found an association between a clinical diagnosis of AD and these hippocampal subregions<sup>22-24</sup> although the presence of ADNP was not confirmed in these studies. This is an important limitation as previous studies have shown similarities between clinical presentation of HS and AD.<sup>25</sup> Therefore, presence of HS pathology in clinical AD cases cannot be excluded. Another line of investigation tying hippocampal atrophy and clinical, but not necessarily pathological, AD is that TDP-43 pathology is a common co-pathology in AD<sup>26,27</sup> and recent studies have clearly demonstrated the effect of TDP-43 pathology on hippocampal atrophy.<sup>28</sup> The results from this study suggest that the association between ADNP and CA1/subiculum volume merits further examination.

HS was related to atrophy of hippocampal subfields in both the group comparisons and in the multiple linear regression model that included all the other neuropathological variables. Furthermore, the within-HS+ group analysis did not reveal a significant difference by either

ADNP or dementia status, suggesting that the effect of HS on atrophy of the hippocampal subfields is strong and independent of ADNP and dementia status. Coupled with the fact that 40% of those with ultimate HS pathology did not have dementia at the time of scan, these results suggest that hippocampal subfield atrophy may be a relatively early imaging biomarker for HS. Given the current lack of HS biomarkers, finding of disproportionate hippocampal atrophy at pre-dementia stage might be a valuable biomarker of this important pathology that often comes into the differential diagnosis of AD and often happens concurrently with ADNP. The co-occurrence of these two pathologies makes distinguishing HS additionally relevant when interpreting the outcomes of clinical trials of AD-targeted therapies, participants often selected based on AD-specific biomarkers.

A high proportion (81%) of the study participants lacked TDP-43 data and therefore, we could not ascertain the relationship between HS and TDP-43 pathology in this database. Previous studies, however, have shown a very high concordance of the two pathologies. TDP-43 has been reported to be present in  $\approx 80\%$  of hippocampal sclerosis sufferers. In fact, some authorities consider HS the most advanced stage of the recently proposed construct Limbic predominant age-related TDP-43 encephalopathy (LATE).<sup>19</sup> Given the above and the fact that high concordance of the two pathologies would have excluded entering both to the same regression models, we do not believe that lack of TDP-43 pathology detracts from the main finding of this study, which is the profound hippocampal atrophy that accompanies hippocampal sclerosis especially localized to the CA1 region of hippocampus and subiculum.

One of the challenges of using the NACC database lies in the heterogeneity of the MRI data stemming from different acquisition parameters across contributing centers. To overcome this, we implemented multiple quality control steps and examined the change in effect sizes when limiting the dataset to more homogeneous scan acquisitions. We also found similar results using two different methods for hippocampal segmentation (FreeSurfer and ASHS). The results suggest that our findings are robust and may become even stronger with higher quality and more homogeneous MRI scans. One limitation of the study is the limited availability of coronal-oblique T2w images of the hippocampal formation, which greatly aids in defining the internal boundaries of the subfields, for most NACC participants: this meant that only 3D T1w MRIs were used for the segmentation of hippocampal subfields. Despite this, previous analyses showed added value and good test-retest reliability of FreeSurfer hippocampal subfield segmentation in both cognitively normal and AD participants when using only 3D T1w images.<sup>29</sup> Another inherent limitation in this study is the potential variability in neuropathological assessments from different contributing ADCs.

In conclusion, we found greater atrophy of the subiculum and CA1 in participants with HS neuropathology compared to those without HS, both with or without ADNP, with moderate-to-strong effect sizes. Importantly, this atrophy pattern was detectable when approximately half the participants were at a pre-dementia stage. Our results suggest that atrophy of these hippocampal subfields may be an early biomarker and thus help with the detection of HS during life. Complete lack of HS biomarkers at present and the increasing importance of this degenerative pathology in our aging population make our finding particularly important.



## Supplementary Material

Refer to Web version on PubMed Central for supplementary material.

## ACKNOWLEDGMENTS

This work was supported by the National Institutes of Aging grant R01AG062706. The NACC database is funded by NIA/NIH Grant U01 AG016976. NACC data are contributed by the NIA-funded ADCs: P30 AG019610 (PI Eric Reiman, MD), P30 AG013846 (PI Neil Kowall, MD), P30 AG062428-01 (PI James Leverenz, MD), P50 AG008702 (PI Scott Small, MD), P50 AG025688 (PI Allan Levey, MD, PhD), P50 AG047266 (PI Todd Golde, MD, PhD), P30 AG010133 (PI Andrew Saykin, PsyD), P50 AG005146 (PI Marilyn Albert, PhD), P30 AG062421-01 (PI Bradley Hyman, MD, PhD), P30 AG062422-01 (PI Ronald Petersen, MD, PhD), P50 AG005138 (PI Mary Sano, PhD), P30 AG008051 (PI Thomas Wisniewski, MD), P30 AG013854 (PI Robert Vassar, PhD), P30 AG008017 (PI Jeffrey Kaye, MD), P30 AG010161 (PI David Bennett, MD), P50 AG047366 (PI Victor Henderson, MD, MS), P30 AG010129 (PI Charles DeCarli, MD), P50 AG016573 (PI Frank LaFerla, PhD), P30 AG062429-01 (PI James Brewer, MD, PhD), P50 AG023501 (PI Bruce Miller, MD), P30 AG035982 (PI Russell Swerdlow, MD), P30 AG028383 (PI Linda Van Eldik, PhD), P30 AG053760 (PI Henry Paulson, MD, PhD), P30 AG010124 (PI John Trojanowski, MD, PhD), P50 AG005133 (PI Oscar Lopez, MD), P50 AG005142 (PI Helena Chui, MD), P30 AG012300 (PI Roger Rosenberg, MD), P30 AG049638 (PI Suzanne Craft, PhD), P50 AG005136 (PI Thomas Grabowski, MD), P30 AG062715-01 (PI Sanjay Asthana, MD, FRCP), P50 AG005681 (PI John Morris, MD), P50 AG047270 (PI Stephen Strittmatter, MD, PhD).

### Funding information

National Institute on Aging, Grant/Award Numbers: R01AG062706, P30 AG019610, P30 AG013846, P30 AG062428-01, P50 AG008702, P50 AG025688, P50 AG047266, P30 AG010133, P50 AG005146, P30 AG062421-01, P30 AG062422-01, P50 AG005138, P30 AG008051, P30 AG013854, P30 AG008017, P30 AG010161, P50 AG047366, P30 AG010129, P50 AG016573, P30 AG062429-01, P50 AG023501, P30 AG035982, P30 AG028383, P30 AG053760, P30 AG010124, P50 AG005133, P50 AG005142, P30 AG012300, P30 AG049638, P50 AG005136, P30 AG062715-01, P50 AG005681, P50 AG047270; National Science Foundation, Grant/Award Number: U01 AG016976

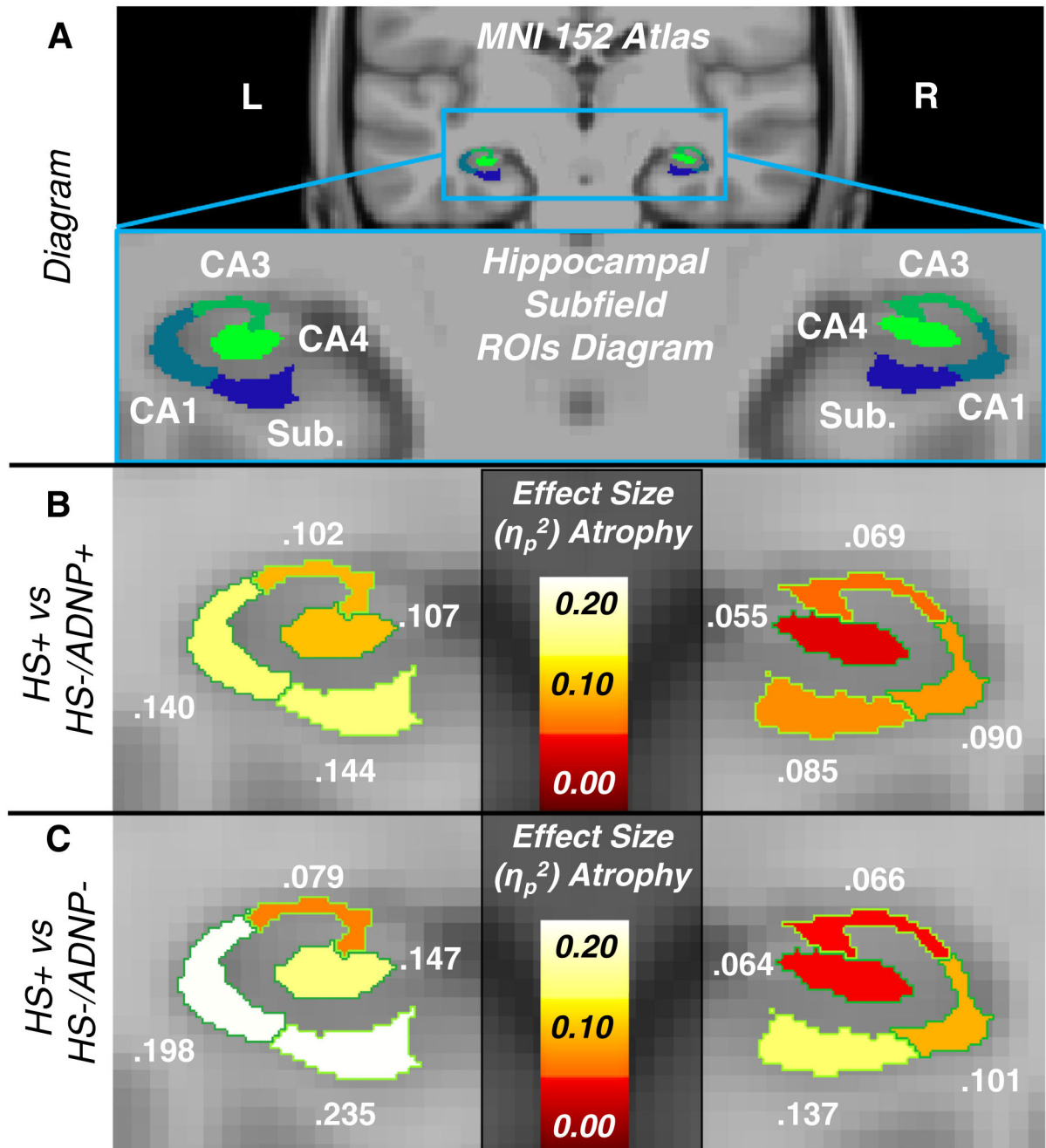
## REFERENCES

1. Kawas CH, Kim RC, Sonnen JA, Bullain SS, T Trieu, MM Corrada. Multiple pathologies are common and related to dementia in the oldest-old: the 90+ Study. *Neurology*. 2015;85:535–542. [PubMed: 26180144]
2. Nag S, Yu L, Capuano AW, et al. Hippocampal sclerosis and TDP-43 pathology in aging and Alzheimer disease. *Ann Neurol*. 2015;77:942–952. [PubMed: 25707479]
3. Kero M, Raunio A, Polvikoski T, Tienari PJ, Paetau A, Myllykangas L. Hippocampal sclerosis in the oldest old: a Finnish population-based study. *J Alzheimers Dis*. 2018;63:263–272. [PubMed: 29614661]
4. Dickson DW, Davies P, Bevona C, et al. Hippocampal sclerosis: a common pathological feature of dementia in very old (>or = 80 years of age) humans. *Acta Neuropathol*. 1994;88:212–221. [PubMed: 7810292]
5. Nelson PT, Smith CD, Abner EL, et al. Hippocampal sclerosis of aging, a prevalent and high-morbidity brain disease. *Acta Neuropathol*. 2013;126:161–177. [PubMed: 23864344]
6. Morris JC, Weintraub S, Chui HC, et al. The Uniform Data Set (UDS): clinical and cognitive variables and descriptive data from Alzheimer Disease Centers. *Alzheimer Dis Assoc Disord*. 2006;20:210–216. [PubMed: 17132964]
7. Beekly DL, Ramos EM, van Belle G, et al. The National Alzheimer's Coordinating Center (NACC) Database: an Alzheimer disease database. *Alzheimer Dis Assoc Disord*. 2004;18:270–277. [PubMed: 15592144]
8. Consensus recommendations for the postmortem diagnosis of Alzheimer's disease Consensus recommendations for the postmortem diagnosis of Alzheimer's disease. The national institute on aging, and reagan institute working group on diagnostic criteria for the neuropathological assessment of Alzheimer's disease. *Neurobiol Aging*. 1997;18:S1–S2. [PubMed: 9330978]

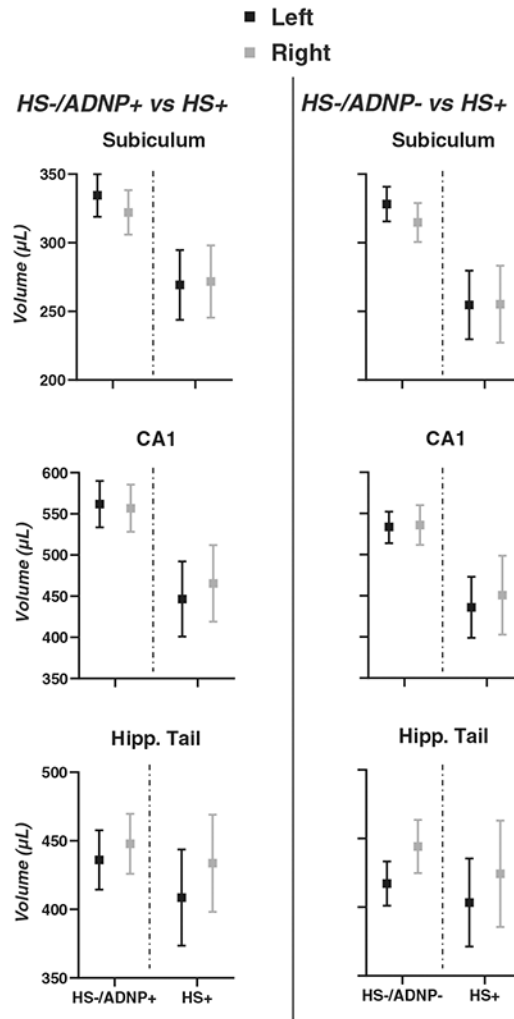
9. Li X, Morgan PS, Ashburner J, Smith J, Rorden C. The first step for neuroimaging data analysis: dICOM to NIFTI conversion. *J Neurosci Methods*. 2016;264:47–56. [PubMed: 26945974]
10. Iglesias JE, Augustinack JC, Nguyen K, et al. A computational atlas of the hippocampal formation using ex vivo, ultra-high resolution MRI: application to adaptive segmentation of in vivo MRI. *Neuroimage*. 2015;115:117–137. [PubMed: 25936807]
11. Xie L, Wisse LEM, Pluta J, et al. Automated segmentation of medial temporal lobe subregions on in vivo T1-weighted MRI in early stages of Alzheimer's disease. *Hum Brain Mapp*. 2019;40:3431–3451. [PubMed: 31034738]
12. Jack CR Jr, Bernstein MA, Fox NC, et al. The Alzheimer's Disease Neuroimaging Initiative (ADNI): mRI methods. *J Magn Reson Imaging*. 2008;27:685–691. [PubMed: 18302232]
13. Cohen J, *Statistical power analysis for the behavioral sciences*: New York: Academic press; 2013.
14. Han X, Jovicich J, Salat D, et al. Reliability of MRI-derived measurements of human cerebral cortical thickness: the effects of field strength, scanner upgrade and manufacturer. *Neuroimage*. 2006;32:180–194. [PubMed: 16651008]
15. Leung KK, Malone IM, Ourselin S, et al. Effects of changing from nonaccelerated to accelerated MRI for follow-up in brain atrophy measurement. *Neuroimage*. 2015;107:46–53. [PubMed: 25481794]
16. Jagust WJ, Zheng L, Harvey DJ, et al. Neuropathological basis of magnetic resonance images in aging and dementia. *Ann Neurol*. 2008;63:72–80. [PubMed: 18157909]
17. Zarow C, Wang L, Chui HC, Weiner MW, Csernansky JG. MRI shows more severe hippocampal atrophy and shape deformation in hippocampal sclerosis than in Alzheimer's disease. *Int J Alzheimers Dis*. 2011;2011:483972. [PubMed: 21547227]
18. Kotrotsou A, Bennett DA, Schneider JA, et al. Ex vivo MR volumetry of human brain hemispheres. *Magn Reson Med*. 2014;71:364–374. [PubMed: 23440751]
19. Yu L, Boyle PA, Dawe RJ, Bennett DA, Arfanakis K, Schneider JA. Contribution of TDP and hippocampal sclerosis to hippocampal volume. *Neurology*. 2020;l:e142–e52.
20. Dawe RJ, Bennett DA, Schneider JA, Arfanakis K. Neuropathologic correlates of hippocampal atrophy in the elderly: a clinical, pathologic, postmortem MRI study. *PLoS One*. 2011;6:e26286. [PubMed: 22043314]
21. Hokkanen SRK, Hunter S, Polvikoski TM, et al. Hippocampal sclerosis, hippocampal neuron loss patterns and TDP-43 in the aged population. *Brain Pathol*. 2018;28:548–559. [PubMed: 28833898]
22. Carlesimo GA, Piras F, Orfei MD, Iorio M, Caltagirone C, Spalletta G. Atrophy of presubiculum and subiculum is the earliest hippocampal anatomical marker of Alzheimer's disease. *Alzheimers Dement (Amst)*. 2015;1:24–32. [PubMed: 27239489]
23. Adler DH, Wisse LEM, Ittyerah R, et al. Characterizing the human hippocampus in aging and Alzheimer's disease using a computational atlas derived from ex vivo MRI and histology. *Proc Natl Acad Sci U S A*. 2018;115:4252–4257. [PubMed: 29592955]
24. de Flores R, La Joie R, Chetelat G. Structural imaging of hippocampal subfields in healthy aging and Alzheimer's disease. *Neuroscience*. 2015;309:29–50. [PubMed: 26306871]
25. Brenowitz WD, Monsell SE, Scimitt FA, Kukull WA, Nelson PT. Hippocampal sclerosis of aging is a key Alzheimer's disease mimic: clinical-pathologic correlations and comparisons with both Alzheimer's disease and non-tauopathic frontotemporal lobar degeneration. *J Alzheimers Dis*. 2014;39:691–702. [PubMed: 24270205]
26. Hu WT, Josephs KA, Knopman DS, et al. Temporal lobar predominance of TDP-43 neuronal cytoplasmic inclusions in Alzheimer disease. *Acta Neuropathol*. 2008;116:215–220. [PubMed: 18592255]
27. Josephs KA, Whitwell JL, Knopman DS, et al. Abnormal TDP-43 immunoreactivity in AD modifies clinicopathologic and radiologic phenotype. *Neurology*. 2008;70:1850–1857. [PubMed: 18401022]
28. Bejanin A, Murray ME, Martin P, et al. Antemortem volume. *Brain*. 2019;l:3621–3635.
29. Worker A, Dima D, Combes A, et al. Test-retest reliability and longitudinal analysis of automated hippocampal subregion volumes in healthy ageing and Alzheimer's disease populations. *Hum Brain Mapp*. 2018;39:1743–1754. [PubMed: 29341323]

### RESEARCH IN CONTEXT

- 1. SYSTEMATIC REVIEW:** We searched the literature using common methods (PubMed and Google Scholar). While some studies have examined the relationship between hippocampal atrophy and hippocampal sclerosis of aging (HS), few examined this relationship focusing on the specific hippocampal formation subfields affected by HS (subiculum and cornu ammonis 1 [CA1]) and of these none examined volumetric differences, instead focusing on deformations in hippocampal surfaces.
- 2. INTERPRETATION:** We found atrophy of the subiculum and CA1 was significantly worse in participants with HS compared to those with or those without Alzheimer’s disease neuropathology (ADNP). Our results suggest that this atrophy pattern can be used as a biomarker for HS during life and to distinguish HS from ADNP.
- 3. FUTURE DIRECTIONS:** Our findings should be replicated by future research. Also, further research should aim to prospectively identify participants with HS during life based on magnetic resonance imaging-detectable atrophy of the subiculum and CA1.

**FIGURE 1.**

Results from group comparisons. A, diagram illustrating regions of interest on a coronal section of MNI 152 atlas and zoomed-in hippocampal formation regions of interest used in this study. B, Heat map of effect sizes for analysis of covariance (ANCOVA) model showing decreased volumes of regions in HS+ compared to HS-/ADNP+. C, Heat map of effect sizes for ANCOVA model showing decreased volumes of regions in HS+ compared to HS-/ADNP-. ADNP, Alzheimer's disease neuropathology; HS, hippocampal sclerosis; CA, cornu ammonis; Sub., subiculum.

**FIGURE 2.**

Marginal means for group comparisons from ANCOVA models adjusted for age, sex, dementia status, years of education, and years from MRI to death. Left, marginal means for HS+ versus HS-/ADNP+ comparison for the subiculum, cornu ammonis 1 (CA1), and hippocampal tail. Right, marginal means for HS+ versus HS-/ADNP- comparison for the subiculum, CA1, and hippocampal tail. Results from the left hemisphere are in black, results from the right hemisphere are in gray. Squares and error bars represent mean and 95% confidence intervals, respectively. ADNP, Alzheimer's disease neuropathology; Hipp, hippocampus; HS, hippocampal sclerosis

**TABLE 1**

Participant characteristics

Variable	Group		P-value	HS+ vs HS-/ ADNP+ P-value
	HS+ (N = 27)	HS-/ADNP- (N = 71)		
Males (%)	13 (48%)	68 (68%)	.2	.06
Age at MRI (SD)	81 (7)	75 (10)	<.001*	.003*
Age at death (SD)	86 (6)	79 (10)	<.001*	.001*
Years MRI to death (SD)	4.4 (2.5)	3.9 (2.1)	.002*	.3
Years of education (SD)	15 (4)	16 (3)	.3	.1
TTV mL (SD)	1539 (197)	1573 (171)	.4	.4
MCI at MRI (%)	11 (41%)	11 (11%)	.002*	<.001*
Dementia at MRI (%)	16 (59%)	87 (87%)	<.001*	.001*
Dementia at last visit (%)	27 (100%)	93 (93%)	<.001*	.2
Lewy bodies (%)	6 (22%)	42 (42%)	.2	.06
CAA (%)	9 (35%) <sup>‡</sup>	48 (48%)	.3	.2
Infarcts (%)	6 (22%)	13 (13%) <sup>‡</sup>	.5	.2
Microinfarcts (%)	4 (15%)	24 (24%)	.5	.3
Hemorrhages (%)	3 (11%)	11 (11%) <sup>‡</sup>	.7	.9
Atherosclerosis (%)	10 (38%) <sup>‡</sup>	43 (43%) <sup>‡</sup>	.6	.6

Notes: Continuous variables (age at MRI, age at death, years from MRI to death, and years of education) are reported as mean and standard deviation within each group and group differences are assessed by analysis of variance, while post hoc comparisons between HS+ and HS-/ADNP+ groups are also reported. Categorical variables (sex, dementia status at MRI, dementia status at death, and pathological variables) are reported as number and percentage within each group and group differences are assessed by Chi-square tests.

<sup>‡</sup>Denotes one participant in group was not assessed for the specific pathology.

<sup>‡</sup>Denotes two participants in group were not assessed for the specific pathology.

\* Denotes statistical significance (P<.05). Abbreviations: ADNP, Alzheimer's disease neuropathology; CAA, cerebral amyloid angiopathy; HS, hippocampal sclerosis; MCI, mild cognitive impairment; MRI, magnetic resonance imaging; SD, standard deviation; TTV, total intracranial volume.

ANCOVA results for group comparisons of volumes for the hippocampal subfields of interest

**TABLE 2**

Hemisphere	Subfield	HS+ vs HS-/ADNP+			HS+ vs HS-/ADNP-				
		F	P	$\eta_p^2$	F	P	$\eta_p^2$		
<i>Left</i>	Subiculum	19.287	<.001*	0.113	0.144	26.423	<.001*	0.182	0.235
	CA1	18.700	<.001*	0.118	0.140	21.188	<.001*	0.156	0.198
	CA3	13.129	<.001*	0.086	0.102	7.379	.008*	0.056	0.079
	CA4	13.751	<.001*	0.085	0.107	14.831	<.001*	0.102	0.147
	<b>Hipp. tail</b>	1.801	.2	0.013	0.015	0.742	.4	0.007	0.009
	<b>Whole hipp.</b>	17.637	<.001*	0.109	0.133	20.003	<.001*	0.140	0.189
<i>Right</i>	Subiculum	10.736	.001*	0.070	0.085	13.691	<.001*	0.109	0.137
	CA1	11.305	.001*	0.077	0.090	9.676	.003*	0.083	0.101
	CA3	8.464	.004*	0.057	0.069	6.049	.02*	0.050	0.066
	CA4	6.718	.01*	0.045	0.055	5.893	.02*	0.047	0.064
	<b>Hipp. tail</b>	0.469	.5	0.004	0.004	1.174	.3	0.011	0.013
	<b>Whole hipp.</b>	9.450	.003*	0.063	0.076	8.862	.004*	0.074	0.093

Notes: HS+ versus HS-/ADNP- and HS+ versus HS-/ADNP+ comparisons.

\* Denotes statistical significance ( $P < .05$ ).

Abbreviations: ADNP: Alzheimer's disease neuropathology; ANCOVA, analysis of covariance; CA, cornu ammonis; Hipp, hippocampus; HS, hippocampal sclerosis.

Effect sizes of group differences in CA1 and subiculum volumes using all scans or only those with more homogeneous acquisitions

**TABLE 3**

N	HS+ vs HS-/ADNP+			HS+ vs HS-/ADNP-		
	Full data	IR only	MPRAGE only	Full data	IR only	MPRAGE only
HS+	27	19	12	27	19	12
HS- Group	100	62	38	71	48	27
<i>Hemisphere</i>						
<i>Subfield</i>	$\eta_p^2$	$\eta_p^2$	$\eta_p^2$	$\eta_p^2$	$\eta_p^2$	$\eta_p^2$
<i>Left</i>						
Subiculum	0.144	0.207	0.312	0.235	0.294	0.209
CA1	0.140	0.171	0.284	0.198	0.255	0.170
<i>Right</i>						
Subiculum	0.085	0.105	0.207	0.137	0.169	0.233
CA1	0.090	0.122	0.216	0.101	0.172	0.247

Abbreviations: ADNP: Alzheimer's disease neuropathology; CA1, cornu ammonis 1; HS: hippocampal sclerosis; IR, inversion recovery; MPRAGE, magnetization prepared rapid acquisition gradient echo.



**TABLE 4**

Multiple linear regression of total subiculum/CA1 volume with respect to demographic and pathological covariates

	Covariate	$\beta$	t	P
<i>Demographic</i>	<i>Age at MRI</i>	-0.233	-3.142	.002*
	<i>Sex</i>	-0.114	-1.594	.1
	<i>Years of education</i>	0.008	0.129	.9
	<i>TIV</i>	0.300	4.208	<.001*
	<i>Dementia</i>	-0.315	-4.642	<.001*
	<i>Years MRI to death</i>	0.045	0.702	.5
<i>Pathological</i>	<i>HS</i>	-0.248	-4.079	<.001*
	<i>ADNP</i>	-0.030	-0.452	.7
	<i>Lewy bodies</i>	-0.048	-0.774	.4
	<i>CAA</i>	-0.052	-0.863	.4
	<i>Atherosclerosis</i>	0.039	0.595	.6
	<i>Infarcts</i>	0.008	0.130	.9
	<i>Microinfarcts</i>	-0.027	-0.415	.7
	<i>Hemorrhages</i>	-0.058	-0.947	.3

\* Denotes statistical significance ( $P < .05$ ). Abbreviations: ADNP, Alzheimer's disease neuropathology; CAA, cerebral amyloid angiopathy; CA1, cornu ammonis 1; HS, hippocampal sclerosis; MRI, magnetic resonance imaging; TIV, total intracranial volume.